Antisense Inhibition of *Escherichia coli* RNase P RNA: Mechanistic Aspects

Heike Gruegelsiepe,[a] Dagmar K. Willkomm,[a] Olga Goudinakis,[b] and Roland K. Hartmann*[a]

The ribonucleoprotein enzyme RNase P catalyzes endonucleolytic 5′-maturation of tRNA primary transcripts in all domains of life. The indispensability of RNase P for bacterial cell growth and the large differences in structure and function between bacterial and eukaryotic RNase P enzymes comply with the basic requirements for a bacterial enzyme to be suitable as a potential novel drug target. We have identified RNA oligonucleotides that start to show an inhibitory effect on bacterial RNase P RNAs of the structural type A (for example, the Escherichia coli *or* Klebsiella pneumoniae *enzymes) at subnanomolar concentrations in our in vitro precursor tRNA (ptRNA) processing assay. These oligonucleotides are directed against the so-called P15 loop region of RNase P RNA known to interact with the 3′-CCA portion of ptRNA substrates. Lead probing experiments demonstrate that a complementary RNA or DNA 14-mer fully invades the P15 loop region and thereby disrupts local structure in the catalytic core of RNase P RNA. Binding of the RNA 14-mer is essentially irreversible because of a very low dissociation rate. The association rate of this oligonucleotide is on the order of $10^4\ M^{-1}\ s^{-1}$ and is thus comparable to those of many other artificial antisense oligonucleotides. The remarkable inhibition efficacy is attributable to the dual effect of direct interference with substrate binding to the RNase P RNA active site and induction of misfolding of the catalytic core of RNase P RNA. Based on our findings, the P15 loop region of bacterial RNase P RNAs of the structural type A can be considered the "Achilles' heel" of the ribozyme and therefore represents a promising target for combatting multiresistant bacterial pathogens.*

Introduction

The ubiquitous enzyme ribonuclease P (RNase P) catalyzes endonucleolytic 5′-maturation of tRNA primary transcripts in all domains of life including eukaryotic organelles.[1–3] Bacterial RNase P enzymes are composed of a catalytic RNA subunit (about 130 kDa in size) and a single small protein (about 13 kDa).[4] The RNA subunit of bacterial enzymes is catalytically active in vitro without the protein subunit but requires elevated salt concentrations for optimum activity to compensate for the absence of the protein.[5] The architecture of human RNase P differs from its bacterial counterparts in many aspects, such as the higher number of protein subunits (10 proteins, 1 RNA),[6] the inactivity of its RNA subunit alone in vitro,[7, 8] and the minimization or even lack of contacts between its RNA subunit and precursor tRNA (ptRNA) substrates.[9] Since RNase P is essential for bacterial growth,[1] the structural and functional differences between human and bacterial RNase P may be exploited to develop novel drugs targeted against bacterial RNase P to control bacterial pathogens at a low risk of interference with human RNase P function. In the preceding report by Willkomm et al.[10] we demonstrated that antisense oligonucleotides designed to target the binding site for the tRNA 3′ CCA moiety in bacterial Type A RNase P RNAs can efficiently block enzyme function. Herein we report the optimization of RNA oligonucleotides targeted at this region. We have identified variants that inhibit *Escherichia coli* or *Klebsiella pneumoniae* RNase P RNAs with K_i (defined as the oligonucleotide concentration required to obtain 50% inhibition of ptRNA cleavage by RNase P RNA) and K_d (dissociation constant) values of around 1 nM under our standard assay conditions. We further characterized the structure of oligonucleotide–RNase P RNA complexes by lead probing[11] and analyzed the kinetics (association and dissociation rate constants, k_{on} and k_{off}, respectively) of oligonucleotide binding to RNase P RNA. According to our data, the P15 loop target region is converted into a hybrid helix involving all 14 nucleotides of the RNA or DNA 14-mer, which results in the disruption of local structure in the catalytic core of RNase P RNA. Binding of the RNA 14-mer is essentially irreversible as a result of a very low dissociation rate. In conclusion, the P15 loop region of bacterial RNase P RNAs of the structural type A can be considered as the "Achilles' heel" of the ribozyme. The remarkable inhibition efficacy of antisense oligonucleotides directed at this region can be attributed to two effects: direct interference with substrate binding to the active site of RNase P RNA and induction of misfolding of the RNA

[a] *Prof. Dr. R. K. Hartmann, H. Gruegelsiepe, Dr. D. K. Willkomm*
Philipps-Universität Marburg
Institut für Pharmazeutische Chemie
Marbacher Weg 6, 35037 Marburg (Germany)
Fax: (+49) 6421-282-5854
E-mail: hartmanr@staff.uni-marburg.de

[b] *O. Goudinakis*
Universität zu Lübeck
Institut für Biochemie
Ratzeburger Allee 160, 23538 Lübeck (Germany)

 DOI: 10.1002/cbic.200300675

catalytic core. Efficient inhibition of the essential ribonucleoprotein enzyme RNase P by an antisense-based strategy directed against the CCA binding region is encouraging and clearly justifies further efforts to explore bacterial RNase P as a target to combat multiresistant bacterial pathogens.

Results

In the preceding paper by Willkomm et al.[10] we reported that a 15-nt-long RNA oligonucleotide (15-mer, Figure 1) inhibits precursor tRNA (ptRNA) processing by *E. coli* RNase P RNA quite efficiently. We provided evidence that inhibition is due to oligonucleotide interaction with the P15 loop region, which prevents ptRNA docking into the active site. The model in Figure 1 predicts that oligonucleotides of the15-mer type invade the P15 loop region at the cost of disrupting local RNase P structure, such as the P15 helix.

Table 1. *Kinetic and thermodynamic parameters for interaction of inhibitor oligonucleotides with* E. coli *RNase P RNA.*[a]

	K_i [nM]	K_d [nM]	k_{off} [h^{-1}]	k_{on} [$M^{-1}s^{-1}$]
RNA 14-mer	2.2 ± 0.6	0.7 ± 0.2	0.016 ± 0.01	0.63×10^4
DNA 14-mer	25 ± 5	2.6 ± 0.4	0.22 ± 0.07	2.3×10^4
RNA 13-mer	2.6 ± 0.8	n.d.[b]	n.d.	n.d.
RNA 15-mer	4.0 ± 1.8	n.d.	n.d.	n.d.
RNA 27-mer	9.4 ± 2.5	n.d.	n.d.	n.d.

[a] Mean values derived from at least three independent experiments are given; for details, see the main text and the Methods section. [b] n.d., not determined.

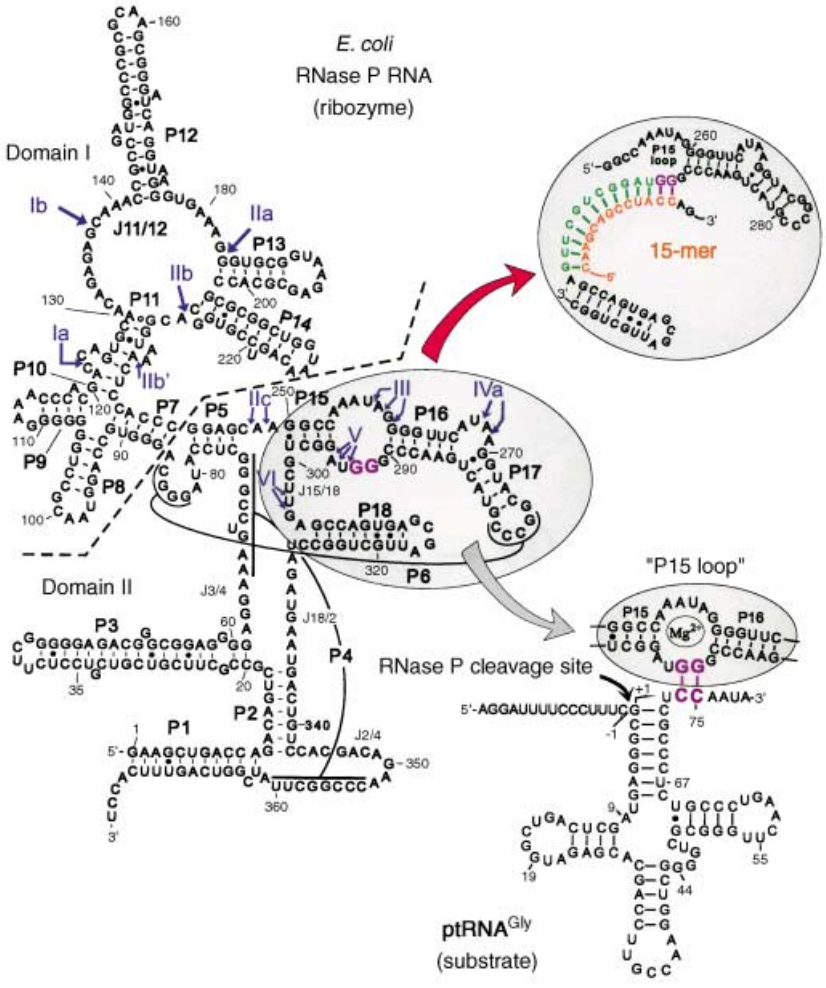

Figure 1. *Secondary structure of* E. coli *RNase P RNA (left) according to Massire et al.[35] The broken line separates the two main structural domains.[36] P, helical regions; J, joining segments named according to the numbers of the helices they connect. Prominent sites of Pb^{2+} hydrolysis are marked (in blue) as in Ciesiolka et al.[11] The grey-shaded oval represents the P15/16 region including G292 and G293 (in magenta); Watson – Crick base pairing of G292/G293 with the CCA motifs of tRNA 3′ termini[37] is depicted for the bacterial $ptRNA^{Gly}$ substrate[38] in the lower right part of the figure; two Mg^{2+} ions bound to the P15 loop have been proposed to be involved in the catalytic process.[39] The red arrow indicates inhibition of* E. coli *RNase P RNA by a 15-mer RNA oligonucleotide complementary (orange nt) to nt 292 – 304 (shown in green and purple) of RNase P RNA.[10] The model in the upper right of the figure predicts that the 15-mer invades the P15 loop region, disrupts helix P15, and anneals to RNase P RNA over the entire region of complementarity.*

Optimization of the 15-mer

The 15-mer, a derivative of our initial RNA oligonucleotide Eco 3′,[10] has a 3′-terminal AG dinucleotide not complementary to the P15 loop region (Figure 1). We therefore tested two variants, one lacking the AG dinucleotide (13-mer) and one with an additional C residue instead (14-mer) to include G291 of the P15 loop in the intermolecular base-pairing interaction (Figure 2 A, B). Both the 13-mer and the 14-mer have slightly lower K_i values than the 15-mer, and the 14-mer proved to be the most efficient inhibitor among all the oligonucleotides tested (Figure 2 A, B; Table 1). We also analyzed whether a 5′ extension of the 14-mer (27-mer) increases inhibition efficacy as a result of the extended complementarity to *E. coli* RNase P RNA. However, this 27-mer is a less potent inhibitor than the 13-, 14-, and 15-mers (Figure 2 A, B; Table 1), which suggests that P18 disruption as a prerequisite for extended intermolecular base pairing was energetically too costly. 5′-terminal shortening of the 14-mer by two or three nucleotides (12-mer and 11-mer) also reduced inhibition efficacy, and a DNA version of the 14-mer was about tenfold less effective than the RNA 14-mer (Figure 2 B, C; Table 1).

Lead probing of inhibitor – RNase P RNA complexes

Pb^{2+}-induced hydrolysis (lead) probing is a powerful technique for the study of RNA structure in vitro and even in vivo.[12] Prominent sites of Pb^{2+}-induced hydrolysis occur at high affinity metal ion binding sites in structured

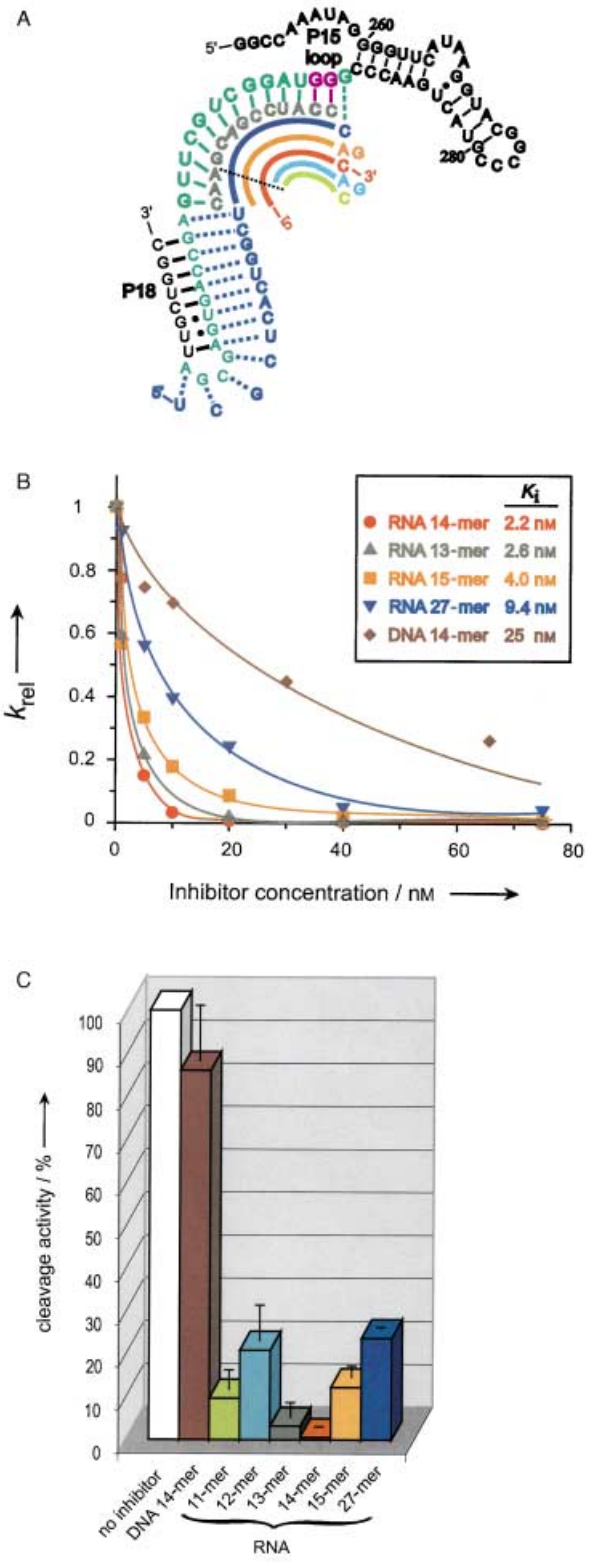

Figure 2. *Antisense inhibition efficacy of RNA oligonucleotides directed against the P15 loop region of* E. coli *RNase P RNA. A) Complexes assumed to be formed between antisense oligonucleotides and RNase P RNA. Nucleotides of the target region are shown in green (nt 292 and 293 in purple); nt in grey represent the 13-mer; the 5′-proximal parts of the other short oligomers are indicated by lines (15-mer, orange; 14-mer, red; 12-mer, light blue; 11-mer, light green); the 27-mer (dark blue) was identical to the 14-mer in its 3′-proximal portion (indicated by a line) but carried a 5′ extension with the potential to pair with the 5′ half of P18, including its apical tetraloop (marked by dotted blue lines). B) Normalized rate (k_{rel}) of ptRNA^{Gly} processing by* E. coli *RNase P RNA as a function of oligonucleotide concentration. K_i values listed in the box represent the oligonucleotide concentration at 50% inhibition relative to the uninhibited reaction (see also Table 1). For assay conditions, see the Methods section. C) Inhibition of cleavage activity by the RNA 11-mer and 12-mer relative to the other oligomers at a twofold excess (20 nM) of oligonucleotide over RNase P RNA (10 nM). Measurements were made by utilizing the same assay as in (B).*

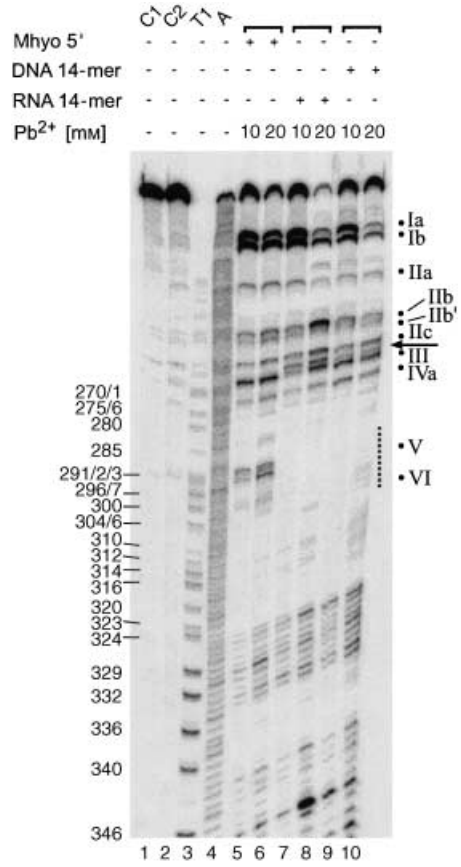

Figure 3. *Pb^{2+}-induced hydrolysis patterns of 3′-^{32}P-labeled* E. coli *RNase P RNA (10 nM) in the presence of either 500 nM RNA 14-mer (Lanes 7, 8), 5 μM DNA 14-mer (Lanes 9, 10), or 5 μM unrelated RNA 25-mer (Mhyo 5′; see the Methods section and ref. [10]) used as a control (Lanes 5, 6). Control lanes 1 and 2: 20000 Cerenkov cpm 3′-^{32}P-labeled* E. coli *RNase P RNA either directly loaded onto the shown 15% polyacrylamide/8 M urea gel (Lane 1) or loaded after incubation in buffer A for 70 min at 37°C (Lane 2); Lanes 3 and 4: limited digestion of 3′-^{32}P-labeled* E. coli *RNase P RNA by RNase T1 (under denaturing conditions; Lane 3) or alkaline hydrolysis (Lane 4). Right: assignment of Pb^{2+}-hydrolysis bands[11, 14] (see also Figure 1); dotted line: area protected by the 14-mers. Left: assignment of G-specific RNase T1 fragments according to the numbering system used for* E. coli *RNase P RNA (Figure 1). For details of the Pb^{2+}-hydrolysis assay, see the Methods section.*

RNA molecules, and less specific minor cleavages are observed in single-stranded flexible regions of RNA.[11] Double-stranded regions are relatively resistant to lead cleavage. Since lead probing has been extensively used to investigate the structure of *E. coli* RNase P RNA,[11, 13–16] we employed this method to analyze the interaction of the most efficient inhibitor, the 14-meric oligonucleotide, with *E. coli* RNase P RNA. Our analysis revealed that the 14-mer (RNA as well as DNA) hybridizes with RNase P RNA over its entire length, as inferred from the suppression of lead hydrolysis in the region spanning nt 291 – 304 of RNase P RNA

(Figure 3, dotted vertical line). In addition, a novel site of lead hydrolysis appeared in the presence of the RNA or DNA 14-mer that corresponds to the 5′-proximal strand of helix P15 that is disrupted upon oligomer invasion (Figure 3, arrow).

Inhibition specificity

RNase P RNA from *E. coli* represents the structural type A among bacterial RNase P enzymes.[17] Two prominent pathogens, *K. pneumoniae* and *Pseudomonas aeruginosa*, also belong to this subclass of RNase P enzymes. RNase P RNAs from *K. pneumoniae* and *E. coli* have identical sequences in the P15 loop region, whereas some nucleotide identities differ in RNase P RNA from *P. aeruginosa* (Figure 4).[4] In the presence of a twofold molar excess of the RNA 14-mer (20 nM) relative to RNase P RNA, the enzymes from *K. pneumoniae* and *E. coli* were inhibited with equally high efficiency. In contrast, inhibition of *P. aeruginosa* RNase P RNA was only moderate under the same conditions (Figure 4), which can be attributed to the successive G·U wobble pair and A–C mismatch in the central region of the hybrid helix. This result suggests that even single mismatches in the 14-bp-long hybrid helix will greatly reduce inhibition efficacy. The 14-mer sequence is unique in the *E. coli* genome (data not shown), which further supports the hypothesis that it is highly specific for the *E. coli* RNase P RNA target.

It will be interesting to test if the efficacy and specificity of the inhibition strategy applies to bacterial type A RNase P enzymes in general. This could be analysed by, for example, reversing the above experiment and using a 14-mer complementary to *P. aeruginosa* RNase P RNA, which would be expected to inhibit this ribozyme more efficiently than that from *E. coli*.

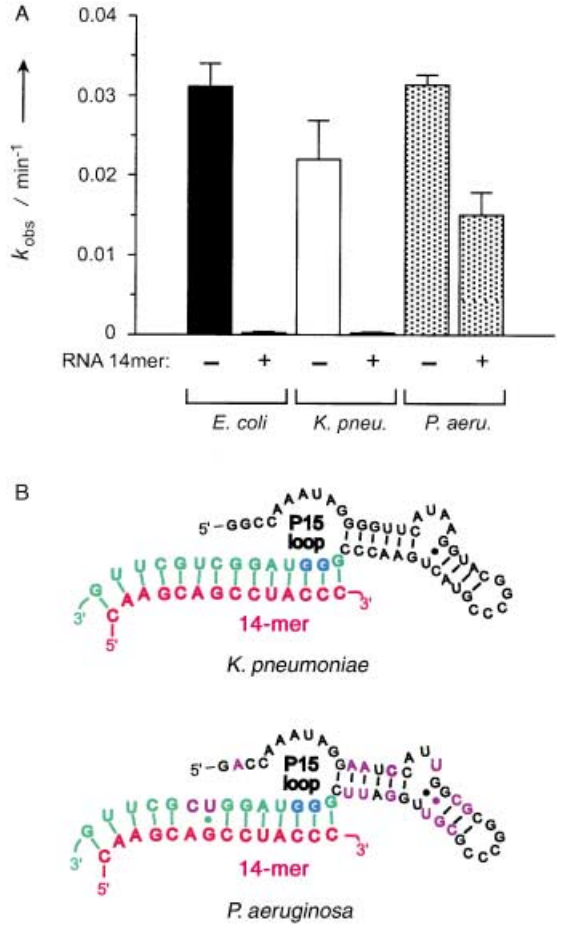

Figure 4. *A) Rate of processing (k_{obs}) of ptRNA^{Gly} (100 nM) by RNase P RNA (10 nM) from* E. coli, K. pneumoniae *(*K. pneu.*), or* P. aeruginosa *(*P. aeru.*) either in the absence or presence of RNA 14-mer (20 nM). Assays were conducted as described in the Methods section. B) Predicted complementarity of the RNA 14-mer (in red) to RNase P RNAs from* K. pneumoniae *and* P. aeruginosa. *RNase P RNAs from* E. coli *and* K. pneumoniae *have identical sequences in the P15 loop region; nucleotide identities that differ in* P. aeruginosa *RNase P RNA relative to the two other bacterial RNase P RNAs are marked in purple; green nucleotides and the conserved G residues (blue; G292/G293 in* E. coli *RNase P RNA) are complementary to the RNA 14-mer.*

Inhibitor association and dissociation

The inhibition efficacy of the 14-mer in its RNA and DNA versions depends on the length of time the inhibitor and RNase P RNA are preincubated together before starting the processing reaction by addition of ptRNA substrate (Figure 5). Maximum inhibition was achieved with both oligomers after 40 min preincubation. Toward an estimate of oligonucleotide association rates and to clarify whether the lower inhibition efficiency of the DNA 14-mer is due to a higher dissociation rate, we first determined the K_d value for 14-mer binding to *E. coli* RNase P RNA by utilizing a spin column assay (see the Methods section). The K_d values for the RNA and DNA 14-mers at room temperature were determined to be 0.7 ± 0.2 nM and 2.6 ± 0.4 nM, respectively (Table 1). Differences between these values and the corresponding K_i values (2.2 nM and 25 nM; Table 1) may to some extent be explained by the higher temperature (37 °C) used in the processing assays.

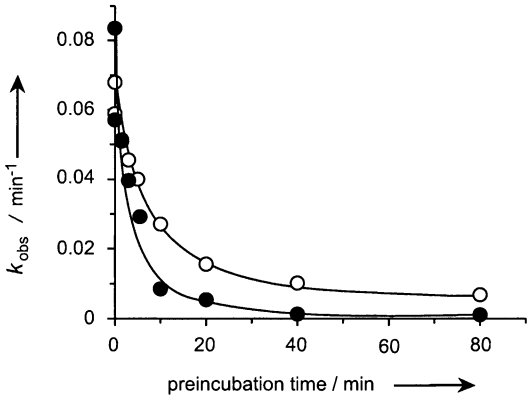

Figure 5. *Inhibition efficacy as a function of oligomer–RNase P RNA preincubation time. The rate of processing (k_{obs}) of ptRNA^{Gly} (100 nM) by* E. coli *RNase P RNA (10 nM) was measured in the presence of RNA 14-mer (10 nM, filled circles) or DNA 14-mer (100 nM, open circles). RNase P RNA was preincubated with RNA or DNA 14-mer in standard assay buffer at 37 °C for the time periods indicated and processing reactions were started by addition of substrate; k_{obs} values represent initial reaction velocities. For further details, see the Methods section.*

We next analyzed the rate (k_{off}) of RNA and DNA 14-mer dissociation from RNase P RNA. For this purpose, trace amounts of 5′-[^{32}P]-labeled 14-mer were incubated for 40 min at 37 °C with *E. coli* RNase P RNA at concentrations close to complex saturation (2 nM in the presence of the RNA 14-mer, 16 nM in the presence of the DNA 14-mer). A 100-fold molar excess (relative to RNase P RNA) of the corresponding unlabeled 14-mer was then added and aliquots were withdrawn at various time points and analyzed for the fraction of 5′-[^{32}P]-labeled 14-mer still bound to RNase P RNA (for details, see the Methods section). In such a set-up, dissociation is essentially irreversible because every radiolabeled oligonucleotide that is released from the complex will be replaced by an unlabeled oligonucleotide molecule. The DNA 14-mer had a k_{off} value of about 0.22 h^{-1}, while the k_{off} value of the RNA 14-mer was about 15-fold lower (0.016 h^{-1}; Figure 6; Table 1). Based on the K_d and k_{off} values, we calculated association rate constants (k_{on}) of $2.3 \times 10^4\,M^{-1}s^{-1}$ for the DNA 14-mer and about $0.6 \times 10^4\,M^{-1}s^{-1}$ for the RNA 14-mer (see the Methods section).

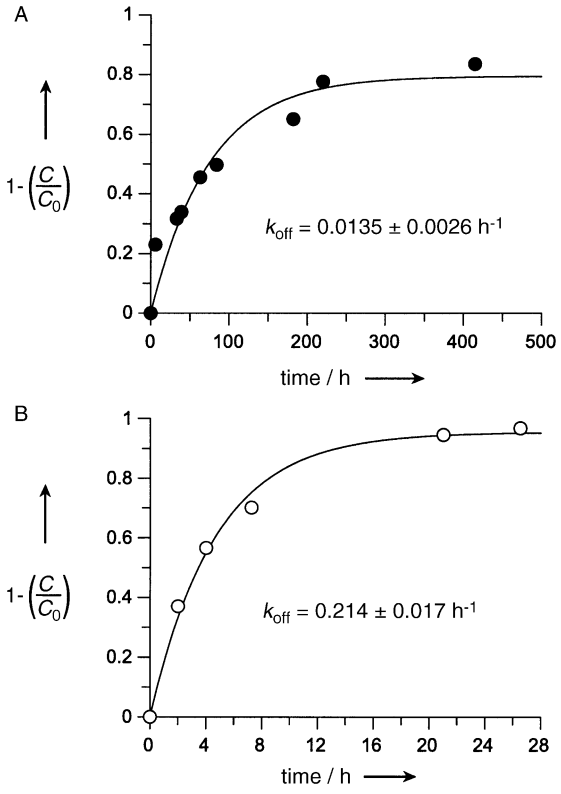

Figure 6. *Determination of dissociation rate constants (k_{off}) for complexes formed between* E. coli *RNase P RNA and either the RNA (A) or DNA (B) 14-mer (data from one representative experiment). A solution of RNase P RNA and radiolabeled oligonucleotide was preincubated to allow the mixture to reach binding equilibrium and was then challenged by a chaser of unlabeled oligonucleotide (100-fold excess over labeled oligomer). Dissociation is essentially irreversible in such an experiment because every radiolabeled oligonucleotide that is released from the complex will be replaced by an unlabeled oligonucleotide molecule. The decrease in the fraction of ^{32}P-oligomer present in the complex as a function of time after addition of the chaser was plotted, and data were fit to a single exponential yielding k_{off} values of 0.0135 ± 0.0026 h^{-1} for the RNA 14-mer (A) and 0.214 ± 0.017 h^{-1} for the DNA 14-mer (B). C_0, maximum fraction of ^{32}P-oligomer in complex with RNase P RNA (time point zero) corrected by the fraction of ^{32}P-oligomer eluting from the spin column in controls lacking RNase P RNA; C, remaining fraction of ^{32}P-oligomer in the complex at different time points after addition of excess unlabeled oligonucleotide, corrected as described for C_0; for further details, see the Methods section.*

Discussion

Mechanism of ribozyme inhibition

Our rational approach has identified a 14-nt-long RNA oligonucleotide that invades the P15 loop region of bacterial RNase P RNA of the structural type A, as found in *E. coli*, *K. pneumoniae*, or *P. aeruginosa*. The RNA and DNA 14-mers hybridized over their entire length with the target (Figure 3), and thereby disrupted the endogenous P15 helix of RNase P RNA. The RNA 14-mer showed the tightest binding (Table 1) to its target in our in vitro assays. The high inhibition efficacy is probably brought about by two effects: 1) direct interference with substrate binding to the active site of RNase P RNA and 2) induction of misfolding of the catalytic core of RNase P RNA. Induction of misfolding by antisense oligonucleotides has recently been explored as a strategy to inhibit autocatalytic removal of a Group I intron from ribosomal RNA transcripts of the human pathogen *Candida albicans*.[18] A single specific region of the intron (the P3/P7 region) was identified that could be driven into an inactive conformation by antisense oligonucleotides. The best K_i values (30 – 150 nM) were obtained with a fully 2′-O-methyl-substituted dodecamer, a dodecamer of identical sequence containing six locked-nucleic-acid (LNA) and six DNA residues, and an octamer fully substituted with LNA residues.[18]

Our assumption that *E. coli* RNase P RNA will be arrested in an inactive conformation upon 14-mer invasion is borne out by mutational studies, in which comparatively minor structural changes introduced into the P15 region (point mutations G300 to C or C301 to G) caused RNase P RNA inactivity in vivo.[15] Similar results were obtained with *E. coli* RNase P RNA variants carrying a deletion of G291 and G292.[19] A G296 to A mutation in P15 was also found to strongly interfere with RNase P RNA function, although in this case in vivo function was not tested.[20]

Kinetics of 14-mer interaction with RNase P RNA

Differences in the K_d values for the DNA and RNA 14-mers were shown to be due to a more than tenfold lower dissociation rate of the RNA 14-mer (Table 1), the value of which was hardly measurable (0.016 h^{-1}). With respect to the in vivo situation, this result may suggest that an RNA 14-mer, once stably bound to an RNase P RNA molecule, will remain almost irreversibly bound to the ribozyme (approximately 10% dissociation after 6 h), possibly over several generation times.

Association rates for the RNA and DNA 14-mer were estimated to be on the order of $10^4\,M^{-1}s^{-1}$, similar to rates measured for other artificial antisense systems.[21] Annealing of the 14-mers to the P15 loop region was associated with disruption of local RNase P RNA structure (Figure 3). It has been shown before that the tightest binding of antisense oligonucleotides occurs at target sites for which target structure disruption is minimal, with

affinity a function of the association rate.[22] Since RNase P RNA is a highly structured RNA, annealing of oligonucleotides of at least 10 nt is predicted to be generally associated with an energetically unfavorable disruption of local or even global structure. Thus, the upper limit for association rates is expected to be on average lower for structured, stable RNAs than for mRNAs, which tend to possess more extended segments that are easily accessible.

Association rate constants on the order of $10^6\,M^{-1}s^{-1}$ were obtained for natural antisense systems in vitro, which apparently correlates with the efficiency of antisense control in vivo.[23] Our initial intention was to mimic the natural CopA – CopT system for inhibition of RNase P RNA and thereby adopt its feature of high association rates.[10] Our results with the best-performing 14-mer demonstrate that this ambitious goal is probably hard to achieve by rational design. Optimization of association rates likely requires target and antisense RNA co-evolution as in natural RNA – RNA interaction systems. Nevertheless, it will be worth investigating whether LNA variants of the 14-mer have improved association kinetics as a result of the "preorganization" of LNA oligonucleotides into an A-helix-like backbone conformation.[24, 25] Interestingly, a so-called U-turn motif in the apical loop of the CopT antisense RNA is also assumed to preform an A-helical conformation of loop nucleotides and may thus improve binding specificity and rate.[23]

Perspectives for in vivo application

The RNA 14-mer is a more efficient inhibitor than shorter variants such as the 12-mer and 11-mer (Figure 2C). We are currently investigating LNA derivatives of the 14-mer because LNA building blocks not only stabilize oligonucleotides against nucleolytic attack but, as mentioned above, also dramatically increase target affinity because of the locking of the C3′-*endo* sugar conformation typical of A-helical RNA-like double strands.[24, 25] As a result, even LNA octamers can elicit very efficient and, surprisingly, specific inhibition effects under conditions where DNA or RNA octamers of the same sequence are inefficient.[18] The reduced length of the efficient LNA oligonucleotides should allow the extent of target structure disruption to be lowered and may thus improve affinity by increasing the association rate.[22] The smaller sizes of the LNA oligomers should also alleviate the problem of bacterial cell entry in approaches relying on exogenous oligonucleotide application.

A peptide nucleic acid (PNA) version of the 14-mer may be another option worth testing, since the neutral backbone of a PNA is assumed to minimize the electrostatic repulsion problem for bacterial cell entry experienced with standard nucleic acids.[26] Covalent attachment of PNA to bioactive peptides that facilitate bacterial cell wall/membrane permeation has been demonstrated to greatly improve exogenous antisense PNA delivery into *E. coli* cells and thus to increase antisense potency by up to two orders of magnitude.[26]

The RNA 14-mer also inhibits the *E. coli* RNase P holoenzyme in vitro.[10] We are currently testing its efficacy in vivo by endogenous expression in *E. coli*. In vivo, several factors may modulate and even improve inhibition efficacy. For example, proteins may accelerate annealing of antisense and target RNAs, as shown for the human tumor suppressor protein p53.[27] Antisense oligonucleotides may also access bacterial RNase P RNA more efficiently during transcription before the ribozyme folds into its compact tertiary structure.

The major obstacle to effective control of bacterial pathogens by antisense-based approaches is the specific targeting of and delivery into pathogenic bacteria. Successful future strategies may utilize chimeric approaches, such as the covalent coupling of modified oligonucleotides to aminoglycosides or arginine-substituted aminoglycosides, or the tethering of oligonucleotides to antimicrobial, membrane-disruptive peptides.[28]

Methods

Inhibitor RNA and DNA oligonucleotides: Oligonucleotides were synthesized or purchased and purified as previously described.[10] The following inhibitor oligonucleotides were employed in the study described herein: RNA Mhyo 5′: 5′-CCUAUUUUUUUUAC-CAAAAUUUAGG;[10] RNA 15-mer: 5′-CAAGCAGCCUACCAG; RNA 13-mer: 5′-CAAGCAGCCUACC; RNA 12-mer: 5′-GCAGCCUACCAG; RNA 11-mer: 5′-GCAGCCUACCC; RNA 27-mer: 5′-UCGCUCACUGGCU-CAAGCAGCCUACCC; RNA 14-mer: 5′-CAAGCAGCCUACCC; DNA 14-mer: 5′-CAAGCAGCCTACCC.

PCR and cloning: For the amplification of the RNase P RNA gene (*rnpB*) of *K. pneumoniae*, total DNA from *K. pneumoniae* strain 3025[29a] served as the template; Primer 1 (5′-CCGGAATTCG**TAATAC-GACTCACTATA**GGAAGCTGACCAGACAGT) and Primer 2 (5′-GCGGGATCctaggTGAAACTGACCGATAAGCC) were used. Genomic DNA of *Pseudonomas aeruginosa* PB 2036 (ATCC 10145; leu-38, res^-, $mod^{+[29b]}$) served as the template for cloning of the corresponding *rnpB* gene, with Primer 3 (5′-CCGGAATTCG**TAATACGACTCACTATA**G-GAGAGTCGATTGGACAGT) and Primer 4 (5′-GCGGGATCcatggGA-GAGTCGATCTATAAGCCGG) for PCR amplification. The 5′ primers 1 and 3 introduced a terminal EcoRI restriction site (underlined) and a T7 promoter (bold), the 3′ primers 2 and 4 BamHI restriction sites (underlined) and StyI or NcoI restriction sites, respectively (lower case letters). PCR fragments were cloned into pUC19 by using EcoRI and BamHI restriction sites, which resulted in plasmids pUCKp*rnpB* and pUCPa*rnpB*. Nucleotide sequences for plasmid inserts were confirmed by dideoxy sequencing (MWG-BIOTECH AG). The resulting *rnpB* clone of *K. pneumoniae* 3025 deviated from that deposited in the RNase P database[4] at positions 42 (C to U exchange), 119 (G to A), and 120 (A to G).

Enzymatic RNA synthesis: The $ptRNA^{Gly}$ substrate and RNase P RNAs were synthesized by T7 run-off transcription essentially as previously described:[30] $ptRNA^{Gly}$ from plasmid pSBpt3′hh linearized with BamHI,[31] *E. coli* RNase P RNA from plasmid pDW98 linearized with BsaAI,[31] *K. pneumoniae* RNase P RNA from plasmid pUCKp*rnpB* linearized with StyI (see above), and *P. aeruginosa* RNase P RNA from plasmid pUCPa*rnpB* linearized with NcoI (see above). *K. pneumoniae* RNase P RNA was also directly transcribed from its genomic PCR amplification product. Transcription reactions for RNase P RNAs were subjected to phenol/chloroform (1:1) extraction, concentrated by EtOH precipitation, and purified by electrophoresis in 7% polyacrylamide/8 M urea gels as previously described.[32]

5′ ^{32}P end labeling of RNAs and DNA oligonucleotides: 5′ end labeling of precursor tRNAs and DNA oligonucleotides with [γ-^{32}P]-

adenosine triphosphate (ATP) and T4 polynucleotide kinase was performed as described previously.[30]

3′ end labeling of RNase P RNA and Pb^{2+}-induced hydrolysis: 3′ [^{32}P] end labeling of *E. coli* RNase P RNA and Pb^{2+}-induced hydrolysis were performed essentially as previously described.[30] Briefly, *E. coli* RNase P RNA (12.5 nM, including 20000 Cerenkov cpm 3′-end-labeled RNase P RNA), U1ΔSm RNA[31] (1.3 μg), and either RNA 14-mer (500 nM) or DNA 14-mer (5 μM) were incubated for 1 h at 37 °C in 1.25 × buffer A (1 × buffer A: 0.1 M $Mg(OAc)_2$, 0.1 M NH_4OAc, 50 mM tris(hydroxymethyl)aminomethane (Tris)-HCl, pH 7.1 at 37 °C) in a reaction volume of 4 μL. Pb^{2+}-hydrolysis reactions were started by adding lead acetate solution (1 μL, 50 or 100 mM), followed by incubation for 10 min at 37 °C. Reactions were stopped by addition of loading buffer[30] (7 μL) supplemented with ethylenediaminetetraacetate (EDTA; 120 mM) and shock freezing in liquid nitrogen.

Limited digestion by RNase T1 and alkaline hydrolysis: Limited digestion by RNase T1 was performed by incubation of *E. coli* RNase P RNA (20000 Cerenkov cpm) in buffer B (20 mM sodium citrate/HCl, 0.2 mM EDTA, 1.4 M urea, pH 5.0) containing RNase T1 (0.06 units; Gibco BRL/Life Technologies) for 5 min at 55 °C (10 μL reaction volume). Reactions were stopped by adding loading buffer (10 μL) followed by shock freezing in liquid nitrogen. For limited alkaline hydrolysis, *E. coli* RNase P RNA (35000 Cerenkov cpm) was boiled for 5 min in $NaHCO_3$ (46 mM) and reactions were stopped by adding an equal volume of loading buffer and freezing in liquid nitrogen.

Kinetics: Processing assays using *E. coli*, *K. pneumoniae*, or *P. aeruginosa* RNase P RNA and data analysis were performed as previously described,[10] if not stated otherwise.

Measurements of K_d and k_{off}: K_d values were measured at room temperature by using the spin column assay.[33, 34] The rate (k_{off}) of RNA 14-mer dissociation from *E. coli* RNase P RNA was determined by competition experiments. Trace amounts of RNA 14-mer (77000 Cerenkov cpm) were preincubated for 40 min at 37 °C with RNase P RNA (2 nM) in processing assay buffer I (0.1 M NH_4OAc, 0.1 M $Mg(OAc)_2$, 50 mM 2-[4-(2-hydroxyethyl)-1-piperazinyl]ethanesulfonic acid (HEPES), pH 7.0) in a total volume of 220 μL. A 20-μL aliquot was withdrawn and analyzed for complex formation by the spin column assay.[33, 34] A solution of the RNA 14-mer (2 μL, 20 μM) was then added to the remaining 200 μL preincubation mixture as competitor, followed by immediate withdrawal of another 20-μL aliquot, which was instantly analyzed by the spin column assay (see above). The aforementioned two 20-μL aliquots, which corresponded to the value of maximum complex formation, gave practically identical yields of complex and the values were therefore averaged. Further 20-μL aliquots were withdrawn at various time points and analyzed correspondingly. A control assay without RNase P RNA was performed in such a way that aliquots were taken and analyzed at the same time points as for the sample with RNase P RNA; this procedure allowed us to confirm that assay conditions remained stable after longer incubation periods. The off rate of the DNA 14-mer was determined according to the same protocol, except that the RNase P concentration was 16 nM and the stock solution of DNA 14-mer competitor had a concentration of 160 μM. For the faster-dissociating DNA 14-mer, very similar results were obtained with a dilution assay. Here, trace amounts of DNA 14-mer (77000 Cerenkov cpm) were preincubated for 40 min at 37 °C with RNase P RNA (500 nM) in buffer I in a total volume of 10 μL. Then the mixture was diluted by addition of more buffer I (190 μL), followed by instant withdrawal and spin column analysis of a 20-μL aliquot corresponding to the value of maximum complex formation. Further 20-μL aliquots were withdrawn at later time points and analyzed correspondingly. A sample without RNase P RNA, used to define the background in the absence of complex formation, served as the control (see above).

Acknowledgements

We are grateful to Markus Paaschburg for kinetic measurements, Uwe Mamat for providing genomic DNA of K. pneumoniae *strain 3025, and Georg Sczakiel for fruitful discussion. This work was supported by the Deutsche Forschungsgemeinschaft (Grant no. HA 1672/7-3).*

Keywords: antisense agents · DNA · oligonucleotides · RNA · RNase P

[1] D. N. Frank, N. Pace, *Annu. Rev. Biochem.* **1998**, *67*, 153 – 180.
[2] S. Altman, L. A. Kirsebom in *The RNA World* (Eds.: R. F. Gesteland, T. Cech, J. F. Atkins), Cold Spring Harbor Laboratory Press, Cold Spring Harbor, NY, 2nd ed. **1999**, pp. 351 – 380.
[3] A. Schön, *FEMS Microbiol. Rev.* **1999**, *23*, 391 – 406.
[4] J. W. Brown, *Nucleic Acids Res.* **1998**, *26*, 351 – 352.
[5] C. Guerrier-Takada, K. Gardier, T. Marsh, N. Pace, S. Altman, *Cell* **1983**, *35*, 849 – 857.
[6] N. Jarrous, *RNA* **2002**, *8*, 1 – 7.
[7] C. Pitulle, M. Garcia-Paris, K. R. Zamudio, N. R. Pace, *Nucleic Acids Res.* **1998**, *26*, 3333 – 3339.
[8] N. Jarrous, S. Altman, *Methods Enzymol.* **2001**, *342*, 93 – 100.
[9] H. L. True, D. W. Celander, *J. Biol. Chem.* **1998**, *273*, 7193 – 7196.
[10] D. K. Willkomm, H. Gruegelsiepe, O. Goudinakis, R. Kretschmer-Kazemir Far, R. Bald, V. A. Erdmann, R. K. Hartmann, *ChemBioChem.* **2003**, *4*, 1041 – 1048.
[11] J. Ciesiolka, W. D. Hardt, J. Schlegl, V. A. Erdmann, R. K. Hartmann, *Eur. J. Biochem.* **1994**, *219*, 49 – 56.
[12] M. Lindell, P. Romby, E. G. Wagner, *RNA* **2002**, *8*, 534 – 541.
[13] A. Tallsjö, S. G. Svärd, J. Kufel, L. A. Kirsebom, *Nucleic Acids Res.* **1993**, *21*, 3927 – 3933.
[14] K. Zito, A. Hüttenhofer, N. R. Pace, *Nucleic Acids Res.* **1993**, *21*, 5916 – 5920.
[15] W. D. Hardt, R. K. Hartmann, *J. Mol. Biol.* **1996**, *259*, 422 – 433.
[16] M. Brännvall, N. E. Mikkelsen, L. A. Kirsebom, *Nucleic Acids Res.* **2001**, *29*, 1426 – 1432.
[17] E. S. Haas, A. B. Banta, J. K. Harris, N. R. Pace, J. W. Brown, *Nucleic Acids Res.* **1996**, *24*, 4775 – 4782.
[18] J. L. Childs, M. D. Disney, D. H. Turner, *Proc. Natl. Acad. Sci. USA* **2002**, *99*, 11091 – 11096.
[19] N. P. Lawrence, S. Altman, *J. Mol. Biol.* **1986**, *191*, 163 – 175.
[20] N. Lumelsky, S. Altman, *J. Mol. Biol.* **1988**, *202*, 443 – 454.
[21] S. Eckardt, P. Romby, G. Sczakiel, *Biochemistry* **1997**, *36*, 12711 – 12721.
[22] W. F. Lima, B. P. Monia, D. J. Ecker, S. M. Freier, *Biochemistry* **1992**, *48*, 12055 – 12061.
[23] F. A. Kolb, H. M. Engdahl, J. G. Slagter-Jager, B. Ehresmann, C. Ehresmann, E. Westhof, E. G. Wagner, P. Romby, *EMBO J.* **2000**, *19*, 5905 – 5915.
[24] M. Petersen, J. Wengel, *Trends Biotechnol.* **2003**, *21*, 74 – 81.
[25] J. Kurreck, *Eur. J. Biochem.* **2003**, *270*, 1628 – 1644.
[26] L. Good, S. K. Awasthi, R. Dryselius, O. Larsson, P. E. Nielsen, *Nat. Biotechnol.* **2001**, *19*, 360 – 364.
[27] W. Nedbal, M. Frey, B. Willemann, H. Zentgraf, G. Sczakiel, *J. Mol. Biol.* **1997**, *266*, 677 – 687.
[28] M. Zasloff, *Nature* **2002**, *415*, 389 – 395.
[29] a) J. M. Warnecke, M. Nitschke, C. E. Moolenaar, E. T. Rietschel, R. K. Hartmann, U. Mamat, *Mol. Microbiol.* **2000**, *36*, 697 – 709; b) M. Bagdasarian, personal communication.
[30] C. Heide, T. Pfeiffer, J. M. Nolan, R. K. Hartmann, *RNA* **1999**, *5*, 102 – 116.
[31] S. Busch, L. A. Kirsebom, H. Notbohm, R. K. Hartmann, *J. Mol. Biol.* **2000**, *299*, 941 – 951.
[32] W. D. Hardt, J. M. Warnecke, V. A. Erdmann, R. K. Hartmann, *EMBO J.* **1995**, *14*, 2935 – 2944.

[33] J. A. Beebe, C. A. Fierke, *Biochemistry* **1994**, *33*, 10294 – 10304.
[34] J. M. Warnecke, R. Held, S. Busch, R. K. Hartmann, *J. Mol. Biol.* **1999**, *290*, 433 – 445.
[35] C. Massire, L. Jaeger, E. Westhof, *J. Mol. Biol.* **1998**, *279*, 773 – 793.
[36] A. Loria, T. Pan, *RNA* **1996**, *2,* 551 – 563.
[37] L. A. Kirsebom, S. G. Svärd, *EMBO J.* **1994**, *13*, 4870 – 4876.
[38] W. D. Hardt, J. Schlegl, V. A. Erdmann, R. K. Hartmann, *Nucleic Acids Res*. **1993**, *21*, 3521 – 3527.
[39] L. A. Kirsebom in *The Many Faces of RNA* (Eds.: D. S. Eggleston, C. D. Prescott, N. D. Pearson), Academic Press, UK, **1998**, pp. 127 – 144.

Received: May 21, 2003 [F 675]

